Soft Matter

PAPER

View Article Online
View Journal

Cite this: DOI: 10.1039/d3sm00687e

Low-intensity mixing process of high molecular weight polymer chains leads to elastomers of long network strands and high fatigue threshold

Xianyang Bao,†[ab] Guodong Nian,†[a] Yakov Kutsovsky,[c] Junsoo Kim,[a] Quan Jiao[a] and Zhigang Suo*[a]

Many polymer networks are prepared by crosslinking polymer chains. The polymer chains and crosslinkers are commonly mixed in internal mixers or roll mills. These intense processes break the polymer chains, lower viscosity, and ease mixing. The resulting polymer networks have short chains and a fatigue threshold of ~100 J m^{-2}. Here, we show that a low-intensity process, a combination of kneading and annealing, preserves long chains, leading to a network of polybutadiene to achieve a fatigue threshold of 440 J m^{-2}. In a network, each chain has multiple crosslinks, which divides the chain into multiple strands. At the ends of the chain are two dangling strands that do not bear the load. The larger the number of crosslinks per chain, the lower the fraction of dangling strands. High fatigue threshold requires long strands, as well as a low fraction of dangling strands. Once intense mixing cuts chains short, each short chain can only have a few crosslinks; the strands are short and the fraction of dangling strands is high—both lower the fatigue threshold. By contrast, a low-intensity mixing process preserves long chains, which can have many crosslinks; the strands are long and the fraction of dangling strands is low—both increase the fatigue threshold. It is hoped that this work will aid the development of fatigue-resistant elastomers.

Received 28th May 2023,
Accepted 13th July 2023

DOI: 10.1039/d3sm00687e

rsc.li/soft-matter-journal

1. Introduction

Some polymer networks are prepared by copolymerizing monomers and crosslinkers in one reactor. Other polymer networks are prepared by crosslinking preexisting polymer chains for two reasons. First, polymers such as natural rubber (NR) and collagen are derived from biological sources.[1,2] Second, polymers such as polybutadiene rubber (BR), styrene-butadiene rubber (SBR), and polydimethylsiloxane (PDMS) are synthesized on a large scale under specialized conditions using dedicated facilities.[3,4]

This paper focuses on preparing polymer networks using polymer chains. An industrial process goes as follows. The polymer chains are mixed with additives, such as crosslinkers, accelerators, antioxidants, and reinforcement particles, to form a compound (Fig. 1(a)). The mixing is commonly conducted in a high intensity process using an internal mixer or roll mill (Fig. 1(b)). To ease mixing, the viscosity of the compound is lowered by making the polymer chains short, either by starting with short polymer chains, or by mastication of long polymer chains during mixing.[5,6] The short polymer chains are then crosslinked into a polymer network (Fig. 1(c)). Such a network of short polymer chains has a low fatigue threshold.[7–9]

Here we use a low-intensity process to preserve long polymer chains, and show that the resulting network has a high fatigue threshold. We choose a species of long polymer chains with a low entanglement molecular weight. We mix the polymer chains and crosslinkers to form a compound using a low-intensity process as follows. We spread a crosslinker on the surface of the polymer sheet, and knead the compound several cycles by folding, compressing, and holding the compound at an elevated temperature. We then further anneal the compound for a prolonged time at an elevated temperature. Kneading preserves the long polymer chains and disperses the crosslinker, whereas annealing relaxes polymer chains and lets them entangle (Fig. 1(d)). After sparsely crosslinking the polymer chains, a network forms in which entanglements greatly outnumber crosslinks (Fig. 1(e)). We demonstrate this approach using high molecular weight polybutadiene chains and dicumyl peroxide (DP) crosslinkers. We show that the

[a] John A. Paulson School of Engineering and Applied Sciences, Harvard University, Cambridge, MA 02138, USA. E-mail: suo@seas.harvard.edu
[b] Centre for Polymer from Renewable Resource, SFSE, South China University of Technology, Guangzhou 510640, China
[c] Expert-in-Residence, Office of Technology Development, Harvard University, Cambridge, MA 02138, USA
† These authors equally contributed to this work.

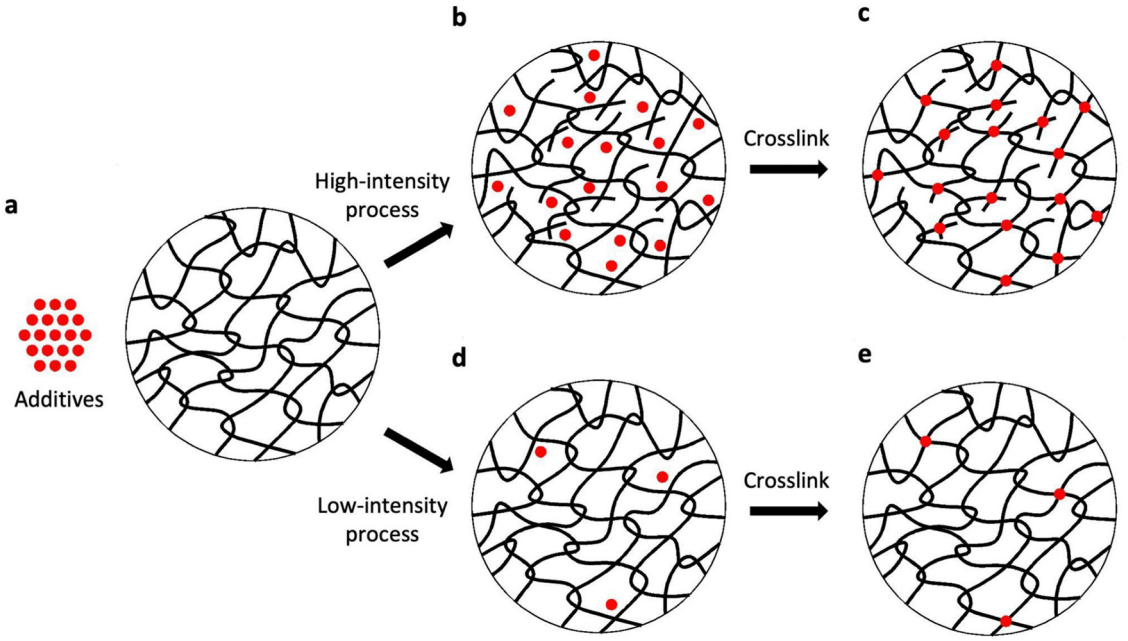

Fig. 1 High-intensity and low-intensity processes of mixing. (a) Polymer chains and additives. (b) The high-intensity process mixes the compound but breaks the polymer chains. (c) After annealing and crosslinking, a short-strand network forms, in which the number of entanglements is comparable to the number of crosslinks. (d) The low-intensity process mixes the compound and preserves the polymer chains. (e) After annealing and crosslinking, a long-strand network forms, in which entanglements greatly outnumber crosslinks.

elastomer has a high modulus, strength, toughness, and fatigue threshold.

2. Effect of the network topology on the fatigue threshold and modulus

Consider the topology of a network (Fig. 2). Each chain has multiple crosslinks, which divide the chain into multiple strands. Each strand at an end of the chain is constrained by only one crosslink, and is called a dangling strand. Each of the other strands of the chain is constrained by two crosslinks, and is not a dangling strand, which we call a network strand. Let N_c be the number of crosslinks per chain on average. The N_c crosslinks divide a chain into $N_c + 1$ strands, of which $N_c - 1$ strands are network strands. Consequently, the fraction of network strands is $\varphi = (N_c - 1)/(N_c + 1)$. For example, a chain having two crosslinks is divided into three strands, and the fraction of network strands is 1/3. As another example, a chain having 10 crosslinks is divided into 11 strands, and the fraction of network strands is 9/11. The larger the number of crosslinks per chain, the higher the fraction of network strands.

Polymer chains also form entanglements. An entanglement between two network strands cannot disentangle before one of them breaks. However, an entanglement between two dangling strands can disentangle without breaking and so can an entanglement between a dangling strand and a network strand.

We will be interested in the load bearing of the network over a time scale in which strands have relaxed. That is, the rate of loading is low compared to the rate of relaxation of the strands. In such a situation, dangling strands do not bear the load, but network strands do. We neglect the effects of network heterogeneities due to crosslinking and some defects such as loops.

When a crack impinges upon a network strand, the strand is pulled in tension, and the tension is transmitted along the length of the strand (Fig. 3). When the strand breaks at a single

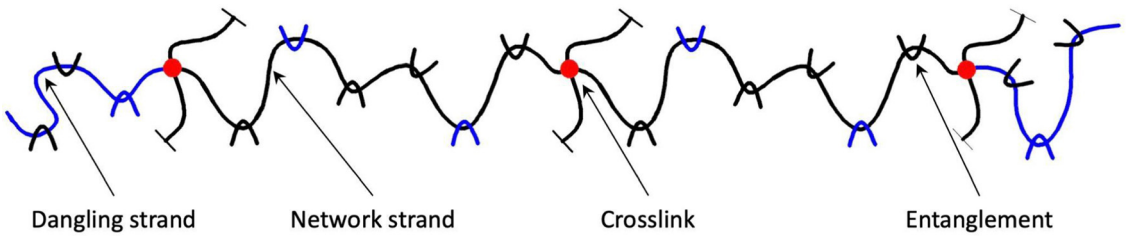

Fig. 2 In a polymer network, crosslinks divide each polymer chain into many strands. Each strand at an end of a chain is constrained by only one crosslink, and is called a dangling strand (blue). Each of the other strands of the chain is constrained by two crosslinks, and is called a network strand (black).

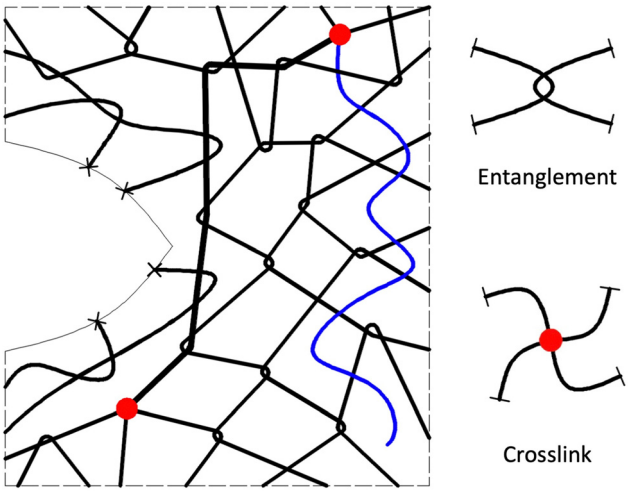

Fig. 3 Dangling strands (blue) do not bear the load, but network strands (black) do. When a crack impinges upon a network strand, the tension is transmitted along the entire strand. The entanglements do not impede the transmission of the tension, but the crosslinks do.

covalent bond, the energy stored in the entire strand is dissipated. Consequently, the longer the strand is, the higher the energy is stored in the strand before the strand breaks, and more energy is dissipated when the strand breaks. According to the Lake–Thomas model, the fatigue threshold of a polymer network scales as follows:[10]

$$G_{th} = \varphi l n^{1/2} J v^{-1} \quad (1)$$

where l is the length of the monomer, n is the number of monomers per strand, J is the chemical energy of a covalent bond along the chain, and v is the volume per bond. Here we modify the equation by multiplying the factor φ. That is, only the network strands contribute to the fatigue threshold.

A high-intensity mixing process cuts chains short. The short chains are then crosslinked into a network. In the network, if each chain has many crosslinks, then every strand will be short, and the network will have a low fatigue threshold. On the other hand, if each chain has a few crosslinks, then the fraction of network strands is low. Consequently, regardless of the number of crosslinks per chain, a network of short chains cannot achieve a high fatigue threshold. By contrast, a low-intensity mixing process preserves long chains. Each long chain can have many crosslinks, such that the strands are long and the fraction of network strands is high. Both increase the fatigue threshold of the network.

Crosslinks and entanglements play different roles in the fatigue threshold of the network.[11–13] Consider a network strand near the breaking point (Fig. 3). When the strand reaches a crosslink, the tension of the strand is transmitted through the crosslink to several other network strands. Consequently, the strand bears higher tension than the other network strands. In this sense, crosslinks concentrate stress. The strand may have many entanglements. At a low strain rate, the entanglements slip readily, and do not impede the transmission of tension along the strand. In this sense, entanglements deconcentrate tension. While dense crosslinks reduce the fatigue threshold, dense entanglements do not. The fatigue threshold scales with the square root of strand length, which is set by crosslinks, but is unaffected by entanglements.[11]

Crosslinks and entanglements play similar roles in the modulus of the network. Both crosslinks and entanglements contribute to the modulus of the network, $G = G_x + G_e$, where G_x is the modulus contributed by crosslinks, and G_e is the plateau modulus of uncrosslinked polymer chains contributed by entanglements. At a low strain rate, dangling strands do not contribute to the modulus. Here, we modify the traditional formula as $G = \varphi(G_x + G_e)$, which can be written as follows:

$$G = \rho RT\varphi(1/M_x + 1/M_e) \quad (2)$$

where ρ is the density of the polymer, R is the universal gas constant, T is the temperature, M_x is the molecular weight of a strand, and M_e is the entanglement molecular weight. Note that $M_x = M_w/(N_c + 1)$, where M_w is the molecular weight of the chain. When crosslinks are greatly outnumbered by entanglements, $M_x \gg M_e$, and each chain is divided into many strands, $N_c \gg 1$, the above equation recovers that of the definition of the entanglement plateau modulus, $G = \rho RT/M_e$. In this limit, the modulus is independent of the crosslink density, as confirmed by a highly entangled elastomer.[11]

3. Low-intensity and high-intensity processes

We choose polybutadiene chains of a high molecular weight of $M_w \sim 602\,000$ g mol^{-1}. Polybutadiene has a low entanglement molecular weight of $M_e \sim 2640$ g mol^{-1}.[14] That is, each polymer chain has about $N_e = M_w/M_e = 228$ entanglements. We dissolve the crosslinker DP in hexane, drip small drops of the solution on the surface of a polybutadiene sheet, and let hexane evaporate in air (Fig. 4(a)). We mix the polymer chains and crosslinkers by two processes: a low-intensity process by kneading in a hot press (Fig. 4(b)), or a high-intensity process by masticating in a roll mill (Fig. 4(d)). Then the compound is annealed at 65 °C overnight to enable the crosslinkers to homogenize further, and polymer chains to relax and entangle. The polymer chains are thermally crosslinked at 155 °C for 25 minutes in a hot press to form a polymer network.

The low-intensity mixing process aims to homogenize the compound without breaking polymer chains (Fig. 4(b)). The chain scission theory indicates that the chain scission depends on the Deborah number (De), which is the ratio of the polymer relaxation time to flow residence time.[15] If $De \ll 1$, the polymer relaxation time is short or the flow residence time is long, so the chain scission would not occur. The short length and low friction of the polymer chains give a short relaxation time. Increasing the temperature or adding a solvent decreases chain friction, resulting in a decreased De from a reduced polymer relaxation time. Polymer chains are mobile without scission if the compound is homogenized within a window of temperature, strain, strain rate, and hold time. After some trial and error, we conduct each cycle of kneading using the following

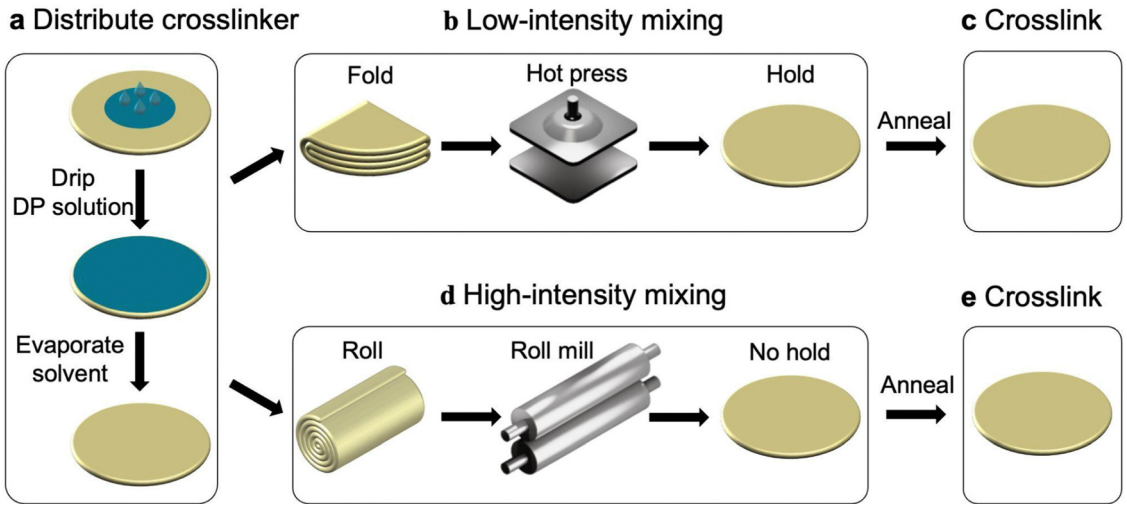

Fig. 4 Two processes to fabricate polymer networks from polymer chains. (a) Distribution of the crosslinker on the surface of the polymer sheet. (b) The low-intensity process mixes the compound by kneading (cycles of fold, hot press, and hold). (c) The mixed compound is annealed and crosslinked. (d) The high-intensity process mixes the compound with a roll mill. (e) The mixed compound is annealed and crosslinked.

steps. Fold a sheet of the polymer twice within a few seconds, hot-press it at 90 °C to its original thickness at a strain rate of $\sim 1\ s^{-1}$, and hold it at the original thickness for 10 minutes to relax the polymer chains. This cycle of kneading is repeated seven times. The combination of a low strain rate and relaxation ensures that kneading minimizes chain scission. Before the cycles of kneading, the heterogeneity is over the original thickness of the polymer sheet (0.6 mm). Then, the heterogeneity is over $4^{-7} = 1/16\,384$ times that of the original thickness (*i.e.*, 37 nm). This nanoscale heterogeneity is small enough to ensure effective homogenization of crosslinkers through diffusion. The mixed compound is annealed at 65 °C for 12 hours, and then crosslinked at 155 °C for 25 minutes (Fig. 4(c)).

By contrast, the high-intensity mixing process aims to illustrate the effect of chain scission (Fig. 4(d)). We use a roll mill to mix the crosslinker and the polymer. Each cycle of the roll-mill consists of the following steps. Roll a sheet of the polymer, put it in between two rigid rolls, and mill. Before milling, the diameter of the polymer sample is 20 mm. The gap between the two rolls is 1 mm, and the two rolls rotate in the same direction at a surface speed of $\sim 0.4\ m\ s^{-1}$. Consequently, the roll mill applies a high strain rate of $\sim 10\ s^{-1}$. The compound is not allowed to rest after each pass of milling, so the tension in polymer chains accumulates cycle by cycle. The milling is repeated 50 times, and the compound increases its temperature to ~60 °C. The combination of high strain rate and large strain causes chain scission–that is, the roll mill masticates the polymer chains. The compound with the shortened chains has a low viscosity, and the roll mill mixes the compound efficiently. The mixed compound is annealed at 65 °C for 12 hours, and then crosslinked at 155 °C for 25 minutes (Fig. 4(e)).

We compare as-received, kneaded, and roll-milled samples with regard to their rheological properties (Fig. 5). All samples are uncrosslinked, and are tested after annealing under the same conditions of 65 °C and 12 hours. Three rheological properties are measured: storage modulus G', loss modulus G'', and steady state viscosity η of the polymer solution.

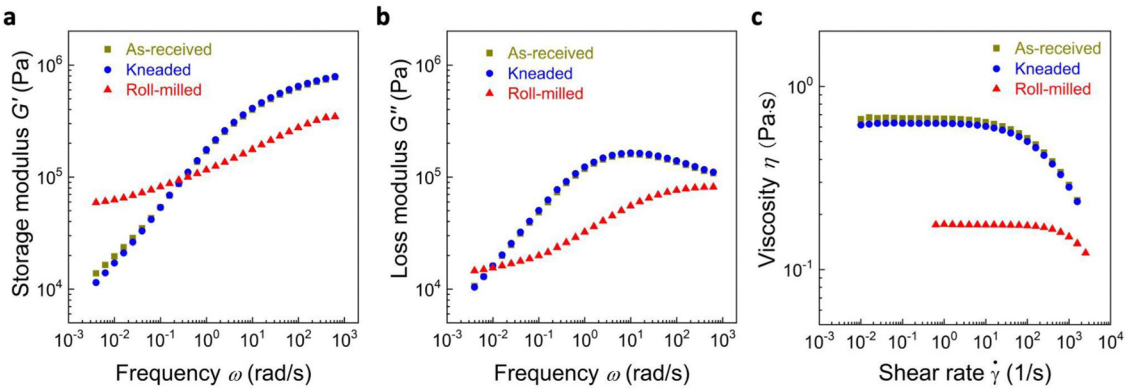

Fig. 5 Rheology of the as-received, kneaded, and roll-milled samples. (a) The storage modulus as a function of frequency. (b) The loss modulus as a function of frequency. (c) Steady-state viscosity of polymer solutions as a function of the shear rate.

For each rheological property, the curves of the as-received and kneaded samples nearly coincide, but they differ markedly from the curve for the roll-milled sample. These results confirm that kneading preserves the polymer chains, but the roll mill breaks them.

More detailed comparisons of rheological curves for the kneaded and roll-milled samples shed additional insight. At low frequencies, the storage modulus G' of the kneaded sample is lower than that of the roll-milled sample (Fig. 5(a)). It is known that the roll mill breaks polymer chains, and the scission produces free radicals, which react to crosslink some polymer chains.[16] At high frequencies, the storage modulus G' of the kneaded sample is higher than that of the roll-milled sample. The modulus at high frequencies is mainly set by entanglements, and short polymer chains disentangle more readily than long chains.[17] The loss modulus G'' of the kneaded sample is higher than that of the roll-milled sample for all frequencies, except for very small frequencies (Fig. 5(b)). Long polymer chains are expected to have a higher loss modulus than short polymer chains. The zero-shear viscosity of the solution of the as-received sample is four times that of the roll-milled sample (Fig. 5(c)). The zero-shear viscosity has a 3.4 power law dependence on molecular weight for an entangled polymer solution,[18] so that the roll mill breaks the as-received polymer chains into two halves. The reduction of the chain length may be underestimated as the broken chains with free radicals can combine to form branched chains which increases the zero-shear viscosity. This result further confirms that the roll mill breaks polymer chains.

4. Effect of the processes on the network topology and the mechanical properties

We then compare the mechanical properties of samples prepared by kneading and roll mill. We prepare samples using the two processes but with the same crosslinker content (r = 0.05 Parts per Hundred Rubber, PHR). For each sample, we measure the stress–stretch curve (Fig. 6(a)). Stretch is defined by the length of a body in the deformed state divided by that in the undeformed state. The kneaded samples have a higher modulus and strength than the roll-milled samples. The two types of samples have comparable stretchability. On loading and unloading, samples prepared by both processes exhibit hysteresis and residual stretch (Fig. 6(b)). We then introduce precracks in the samples made by the two processes. We measure toughness by monotonically stretching the samples to break. The samples of the two types have comparable toughness. We measure crack growth per cycle by cyclically stretching the samples to a fixed amplitude of energy release rate. For each type of sample, the crack growth per cycle increases with the amplitude of the energy release rate (Fig. 6(c)). At the same amplitude of the energy release rate, the crack growth per cycle is smaller in the kneaded sample than in the roll-milled sample. For samples of each type, an amplitude of energy release rate exists, called the fatigue threshold, below which the crack does not grow. The kneaded sample has a higher fatigue threshold than the roll-milled sample. Overall, the

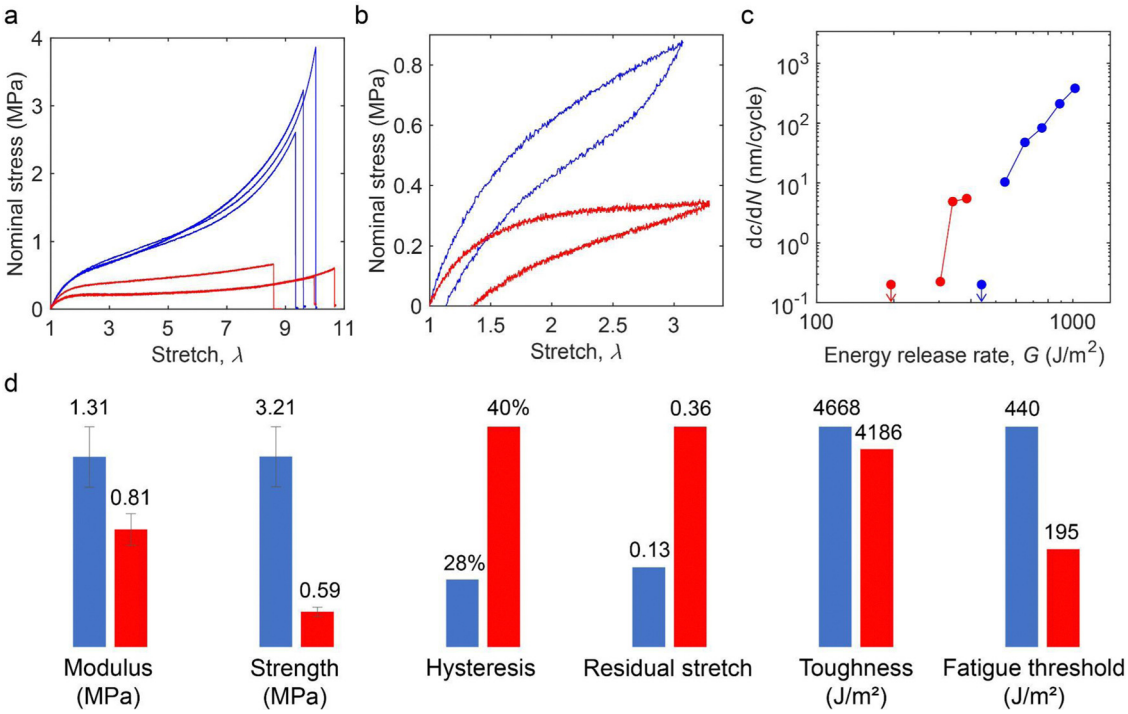

Fig. 6 Properties of polymer networks prepared by kneading (blue) and roll mill (red). Both networks have the same crosslinker content, r = 0.05 PHR. (a) Stress–stretch curves. For each process, three samples are tested. (b) Load–unload curves. (c) Crack growth per cycle dc/dN as a function of the amplitude of the energy release rate. (d) Comparison of mechanical properties between polymer networks prepared by two processes.

kneaded sample has better mechanical properties than the roll-milled sample (Fig. 6(d)).

The difference in the properties of the two types of polymer networks is related to their molecular structures. For the kneaded sample, each polymer chain has a number of entanglements of $N_e = 228$. Entanglements markedly outnumber the crosslinks, $N_e/N_c = 21$ (see the crosslinking process in the Experimental section). For the roll-milled sample, the polymer chain is shortened by mastication. We recall that the mastication from the roll mill breaks the as-received polymer chains into two halves. Thus, the masticated polymer chains are still long enough, and have the same entanglement molecular weight as the as-received polymer chains. The above estimates indicate that entanglements, not crosslinks, set the moduli of both kneaded and roll-milled samples. Samples prepared by the two processes have the same entanglement density. Yet, we find that the modulus is 1.31 MPa for the kneaded sample, but is 0.81 MPa for the roll-milled sample, giving a ratio of 1.6. We interpret this difference as follows.

As discussed in section 2, the modulus of a network also depends on the fraction of network strands, $\varphi = (N_c - 1)/(N_c + 1)$. Mastication cuts chains into two halves, so that the fraction of network strands is 0.82 for the kneaded sample, but 0.67 for the roll-milled sample. As noted before, an entanglement between two network strands cannot disentangle, but an entanglement between two dangling strands can (Fig. 2) and so can an entanglement between a dangling strand and a network strand. When the network is stretched at a low strain rate, only the network strands bear the load (eqn (2)), so the estimated ratio of moduli of the two types of samples is $0.82/0.67 = 1.2$, which is close to the measured ratio given above. The numerical similarity may be fortuitous, but the molecular picture describes a reason that a highly entangled polymer network reduces the modulus when chains are short.

We now examine the relationship between toughness and hysteresis. Following Wang *et al.*,[19] we define hysteresis by the ratio of the area between the loading curve and the unloading curve divided by the area under the loading curve. This definition of hysteresis depends on the stretch, and applies to any large stretch. In this paper, we set the amplitude stretch to be three. By contrast, a traditional measure of hysteresis, the ratio of the loss modulus to the storage modulus, applies to small deformation. The two measures of hysteresis may rank materials differently. The roll-milled sample shows a higher hysteresis than the kneaded sample. This difference is also due to different fractions of dangling strands in the two polymer networks.

Although the two polymer networks have different molecular structures, their toughnesses are comparable. The toughness of a polymer network comes from a synergy between strand scission and strand slip. At a crack tip, before a polymer strand between two crosslinks breaks, the tension is transmitted along the entire length of the strand. When the strand breaks, the tension in the entire strand is released. This picture is represented in the Lake–Thomas model.[10] Off the crack plane, deformation causes polymer strands to slip. As the polymer strand breaks, the crack advances, and the hysteresis due to the strand slip also dissipates energy and contributes to toughness. Because the kneaded sample has lower hysteresis than the roll-milled sample, the energy dissipation contributes less to the toughness of the kneaded sample than to the toughness of the roll-milled sample.

By contrast, the fatigue threshold comes from strand scission, not from strand slip.[10] The kneaded sample is more fatigue-resistant than the roll-milled sample. Upon cyclic stretch, network strands bear the load, but dangling strands slip out and cannot bear the load. The kneaded sample has a higher fraction of network strands (0.82) than the roll-milled sample (0.67). Based on the modified Lake–Thomas model (eqn (1)), the fatigue threshold is proportional to the fraction of network strands. According to this model, the ratio of the fatigue thresholds of the two networks is 1.2. The ratio of the measured fatigue thresholds of the two networks is 2.26.

As noted above, toughness comes from both strand scission and strand slip, but fatigue threshold comes from only strand scission. For example, the kneaded network has a toughness of 4668 J m^{-2} and a fatigue threshold of 440 J m^{-2}. The latter value is taken to be the contribution of strand scission alone. However, the relatively low toughness due to strand scission alone sets high stress in a large volume of networks around the crack tip. In this large volume, the high stress causes strand slip, which greatly contributes to toughness. Consequently, the contributions to toughness by strand scission and strand slip are synergetic. The synergy between crack bridging and background inelastic deformation has been extensively modeled in many materials.[20] The synergy of strand scission and strand slip in the present system has not been modeled.

We next prepare two networks by kneading and by roll mill to have a comparable modulus. The former has a crosslinker content of 0.05 PHR, and the latter has a crosslinker content of 0.1 PHR. As shown in the stress–stretch curves (Fig. 7(a)), the roll-milled samples have a similar modulus to the kneaded samples. The strength of the roll-milled samples is still much lower than that of the kneaded samples. The hysteresis and residual stretch are comparable in the two samples (Fig. 7(b)). The toughness of the kneaded sample is much higher than the roll-milled sample. We further compare the fatigue behavior of both polymer networks. At the same amplitude of energy release rate, the roll-milled sample shows a much larger crack growth per cycle than the kneaded sample (Fig. 7(c)). The measured fatigue threshold of the roll-milled sample is much lower than that of the kneaded sample. Overall, even though the modulus values of the two samples are similar, the extreme properties of the roll-milled samples are much lower than those of the kneaded samples (Fig. 7(d)).

As the crosslinker content is doubled in the roll-milled sample, the number of entanglements per strand of the roll-milled network becomes 10 and the weight fraction of network strands becomes 0.82. We recall the kneaded network, the number of entanglements per strand is 21 and the weight fraction of network strands is 0.82. The modulus of either network is still set by entanglements between network strands, and the weight fractions of the network strands in the two

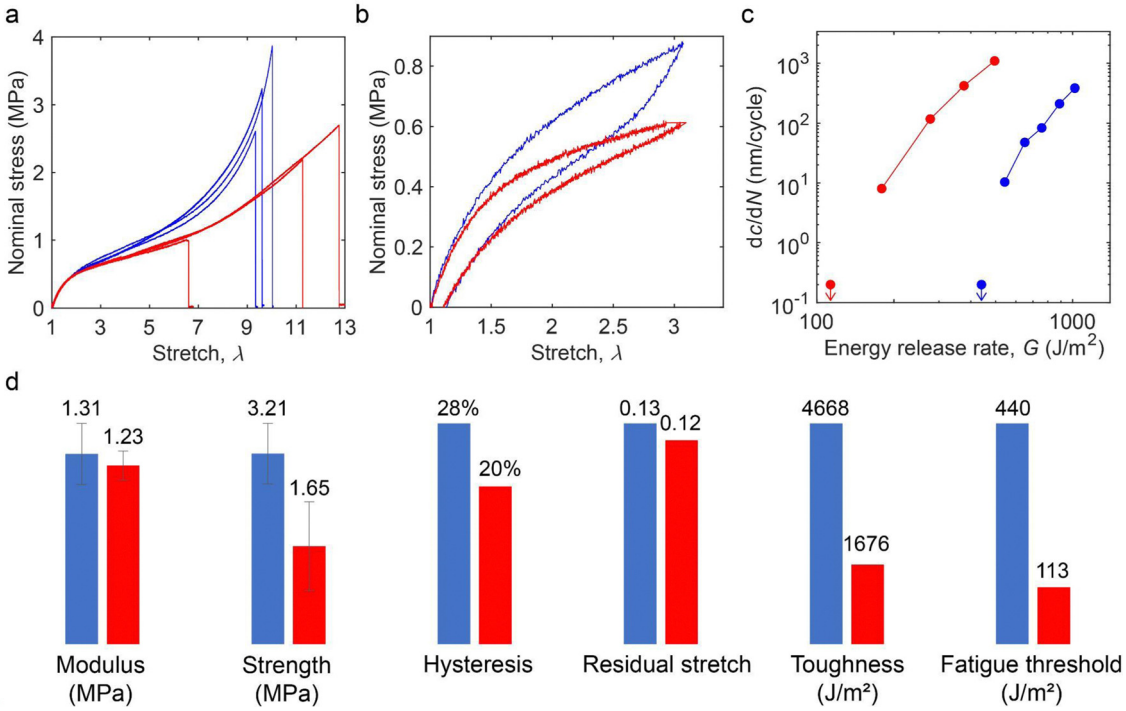

Fig. 7 Properties of the long-strand polymer network prepared by kneading (blue, r = 0.05 PHR) and the short-strand polymer network prepared by roll mill (red, r = 0.1 PHR). The different crosslinker contents are chosen such that the two networks have a comparable modulus. (a) Stress–stretch curves. (b) Load–unload curves. (c) Crack propagation per cycle dc/dN as a function of the amplitude of energy release rate G. (d) Comparison of mechanical properties between two networks.

networks are comparable. Therefore, the roll-milled sample has a comparable modulus to the kneaded sample. The kneaded sample has longer strands than the roll-milled sample, so the fatigue threshold of the roll-milled sample is much smaller than that of the kneaded sample. The former has a larger contribution of strand scission to the toughness than the latter. The contribution of strand scission to the toughness is amplified by the energy dissipation indicated by hysteresis. The hysteresis is comparable in both samples. Consequently, the synergistic contribution of strand scission and strand slip to the toughness in the kneaded sample is higher than that in the roll-milled sample.

5. Effect of the crosslink density on the network topology and the mechanical properties

We next prepared kneaded polymer networks with various crosslinker contents, and measured the stress–stretch curves of these networks (Fig. 8(a)). As the crosslinker content increases, the modulus increases (Fig. 8(b)), the stretchability decreases (Fig. 8(c)), but the strength does not change monotonically (Fig. 8(d)). We interpret these trends as follows.

As the crosslinker content increases, a network forms with shorter strands, and each strand has fewer entanglements. At the crosslinker content r = 0.01 PHR, each polymer chain has about three strands, of which two are dangling–that is, two thirds of the polymer network does not bear the load. Each polymer strand contains about 100 entanglements, so the modulus of the network is set by the entanglements in the network strands. The network has a low modulus because of the low fraction of network strands, and large stretchability because of long strands.

At the crosslinker content r = 0.1 PHR, each polymer chain has about 22 strands, of which two are dangling–that is, 9% of the polymer network does not bear the load. Each strand has $\sim$10 entanglements, so the modulus of the network is still set by the entanglements in the network strands. This increase in the crosslinker content increases the modulus, but decreases stretchability.

At the crosslinker content r = 1.0 PHR, each polymer chain has about 220 strands, of which two are dangling–that is, 1% of the polymer network does not bear the load. Each strand has $\sim$1 entanglements, so that the modulus of the network is set by both the entanglements and crosslinks. Most strands of this network are load bearing. This increase in the crosslinker content increases the modulus, but decreases the stretchability.

We next turn our attention to the nonmonotonic dependence of strength on the crosslinker content (Fig. 8(d)). Before critical strand breaks, tension is transmitted along the entire length of the strand–that is, the entanglements slip readily and deconcentrate tension. By contrast, the tension of the strand is transmitted across a crosslink to multiple strands–that is, the crosslink does not slip and concentrates tension.

At a low crosslinker content, most polymer strands are dangling and do not bear the load, and the strength is low.

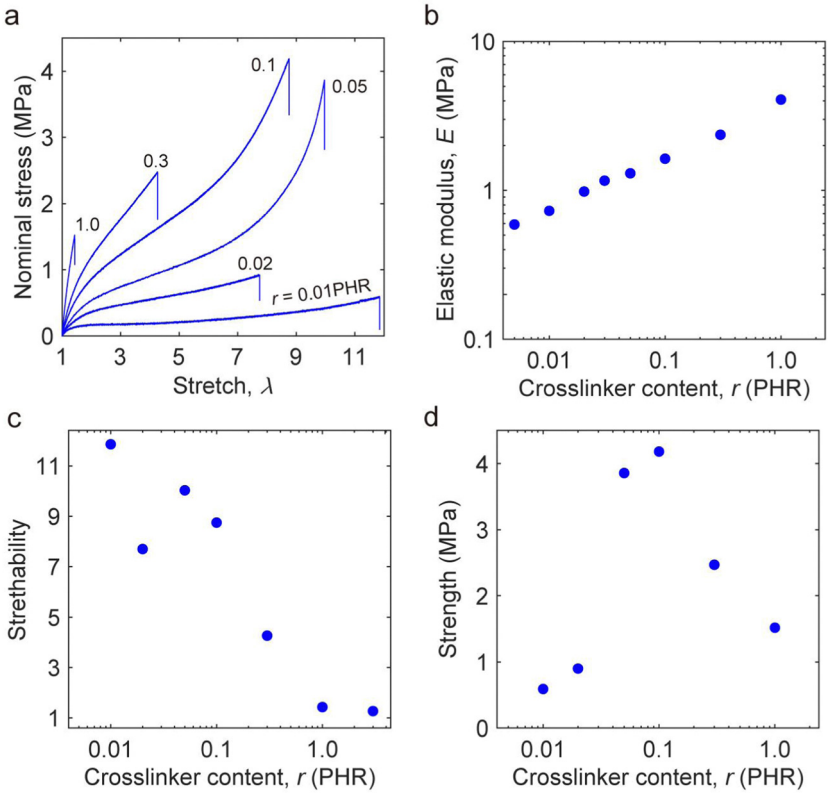

Fig. 8 Properties of the kneaded polymer networks of various crosslinker contents. (a) Stress–stretch curves. (b) Modulus. (c) Stretchability. (d) Strength.

At an intermediate crosslinker content, most polymer strands bear the load, and each strand is still long and contains many entanglements. The network of long strands deconcentrates stress, and increases the strength. At a high crosslinker content, most polymer strands bear the load, and each strand is short and contains few entanglements. The network of extremely short strands concentrates stress, and lowers the strength.

We observe that the strength of each of these polymer networks is on the order of 1 MPa (Fig. 8(d)), which is much smaller than the covalent bond strength, which is on the order of 10 GPa. This dramatic difference indicates that, when a polymer network is near fracture, only a tiny fraction of polymer strands bear the strength of covalent bonds, and most other polymer strands bear the low load of entropic elasticity.[21] This behavior is consistent with the force-displacement behavior of a single polymer strand, measured individually by atomic force microscopy.[22] The force-displacement curve is J-shaped. The force is at the low level of entropic elasticity for a wide range of displacement, but approaches the high level of covalent bond strength for an extremely narrow range of displacement. The average energy of entropic elasticity is on the order of kT, which is 1/40 eV at room temperature. The covalent bond energy is several eV.

We next measure the load–unload curves of the kneaded polymer networks of various crosslinker contents (Fig. 9(a)). As the crosslinker content increases, the polymer strands become

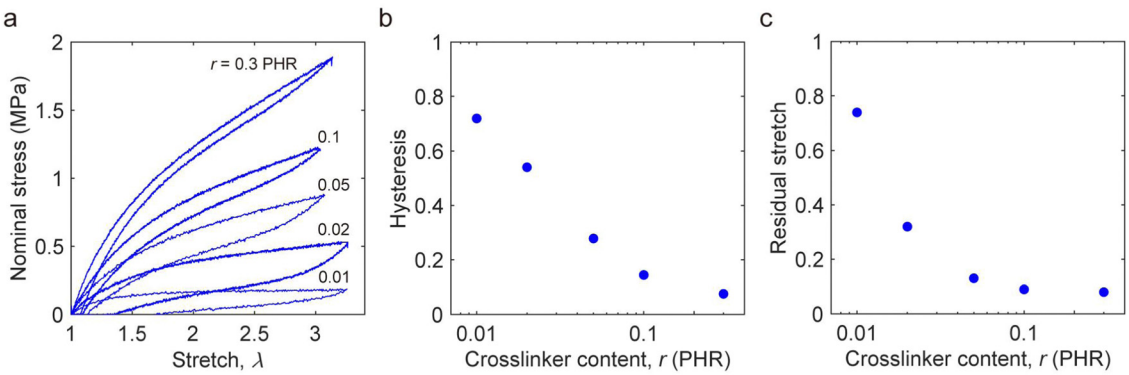

Fig. 9 Kneaded polymer networks of various crosslinker contents subject to load and unload. (a) Load–unload curves. (b) Hysteresis. (c) Residual stretch.

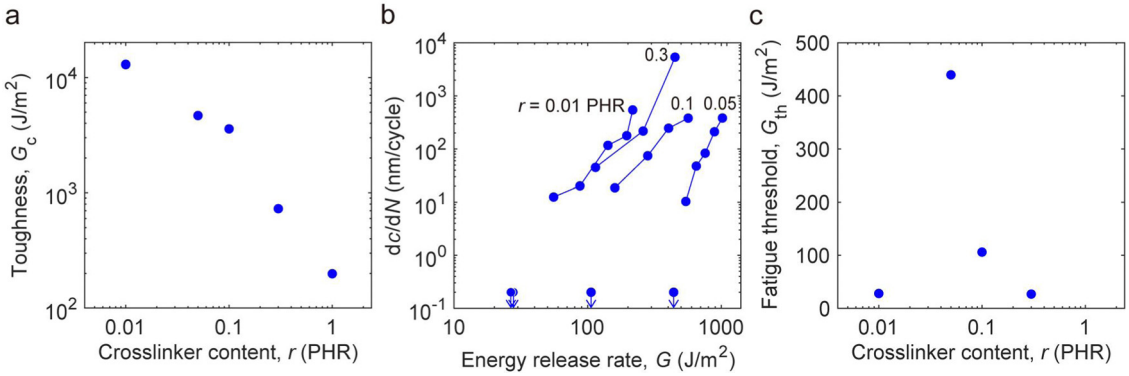

Fig. 10 Toughness and fatigue resistance of kneaded polymer networks of various crosslinker contents. (a) Toughness G_c. (b) Crack growth per cycle dc/dN *vs.* amplitude of energy release rate G. (c) Fatigue threshold G_{th}.

shorter, and the fraction of dangling strands becomes smaller. The polymer network of shorter strands and a smaller fraction of dangling strands require a larger force to load, and is more reversible on unloading. This picture explains that, as the crosslinker content increases, both hysteresis (Fig. 9(b)) and residual stretch (Fig. 9(c)) decrease.

We also measure the toughness and fatigue resistance of the kneaded polymer networks of various crosslinker contents. As the crosslinker content increases, toughness decreases (Fig. 10(a)). For a polymer network of a given crosslinker content, the crack growth per cycle increases with the amplitude of the energy release rate (Fig. 10(b)). However, at a given crack growth per cycle, the amplitude of the energy release rate does not monotonically change with the crosslinker content. As the crosslinker content increases, the fatigue threshold increases, peaks, and decreases (Fig. 10(c)). We interpret these trends as follows.

The toughness of the polymer network comes from a synergy between strand scission and strand slip. As the crosslinker content increases, both the strand length and the hysteresis decrease. A longer strand stores more energy before scission, and causes more hysteresis by slip. Consequently, the synergy of strand scission and strand slip makes toughness higher.

The fatigue threshold comes from strand scission, not from strand slip. As the crosslinker content increases from 0.01 PHR to 0.05 PHR, the fraction of dangling strands decreases, and the fraction of network strands increases from 33% to 82%, so that the fatigue threshold increases. As the crosslinker content further increases to 0.3 PHR, the fraction of dangling strands decreases a little but the length of the strand is much reduced, so that the fatigue threshold decreases.

6. Conclusion

In summary, we show that a low-intensity process, a combination of kneading and annealing, preserves long polymer chains. Long polymer chains enable a network of long strands and a low fraction of the dangling strands, leading to a high fatigue threshold. In such a network, entanglements outnumber crosslinks, so that the modulus is maintained by the dense entanglements. By contrast, the traditional high-intensity process by roll mill breaks polymer chains, leading to a network of short polymer chains. The network of short polymer chains shows a low fatigue threshold regardless of crosslink density. Dense crosslinks shorten polymer strands, whereas sparse crosslinks increase the fraction of dangling polymer strands. Both make the fatigue threshold low.

To improve the efficiency of the low intensity process for large scale throughput, we give three suggestions. First, the process should start with a polymer emulsion. The mixing of the polymer emulsion and additives could enable high efficiency without chain scission. Second, a rubber dispersion kneader should be employed to knead the polymer. The dispersion kneader can provide a low intensity at a long time and high temperature, both of which are beneficial for avoiding chain scission. Third, the processing procedure should be optimized to reduce cycles of kneading, holding time, and annealing time. Small particles of polymers and small particles of additives were premixed, so that fewer cycles of kneading are needed to reach the nanoscale heterogeneity of the compound. The temperature was increased to promote the thermal motion of polymer chains and diffusion of additives but below the activation temperature of the thermal initiator, so that the holding time and annealing time can be much reduced. Pre-existing polymers are commonly used to manufacture tires. Tires of high molecular weight polymers are under development to improve durability. Tire rubber systems also require a significant amount of reinforcing fillers such as fumed silica or carbon black. Hysteresis and fatigue behavior observed in such systems (*e.g.* the ''Mullins effect'') is correlated with the disruption of polymer–filler interactions. The effect of long-chain polymer–filler interactions on the fatigue behavior of particle-reinforced networks will be reported elsewhere. We hope this study provides insight into the development of stiff and fatigue-resistant elastomers.

7. Experimental section

Materials

Polybutadiene rubber (BR; Buna® CB 22; *Cis* 1,4 content > 96; Mooney Viscosity: 63 MU, which approximately corresponds to

a molecular weight of $M_w \sim 602\,000$ g mol^{-1})[23] is kindly provided by ARLANXEO. Dicumyl peroxide (DP), hexane, and phenyloctane are purchased from Sigma-Aldrich and used without further purification.

Low-intensity process

3.5 g of as-received polybutadiene was hot-pressed into a film with a thickness of 0.6 mm at 90 °C. 0.5 mL of hexane solution of DP was evenly dropped onto the surface of the polybutadiene film to form a compound. The compound is left in the air for ten minutes at room temperature for hexane to evaporate. We fold the compound twice, once horizontally and once vertically. The compound is put between two aluminum plates with a 0.6 mm-thick Teflon spacer, compressed at a rate of 5 mm s^{-1}, and then held for 10 minutes at 90 °C. The compound becomes a thin film with the thickness of the spacer. Folding the compound twice and compressing it once constitute a cycle of kneading. The kneading process is repeated seven times. Then the compound is annealed in an oven for 12 hours at 65 °C.

High-intensity process

Polybutadiene and DP are mixed using a two-roll mill. The gap between two rolls of the mill is set as 1 mm. The milling is repeated 50 times. Then the compound is annealed in the oven for 12 hours at 65 °C.

Crosslinking process

After the low-intensity or high-intensity process, the compound is left between the aluminum plates for 25 minutes at 155 °C for crosslinking. Since DP is miscible with polybutadiene, DP is molecularly distributed without phase separation. At 155 °C, DP decomposes into two primary free radicals.[24] The primary free radical abstracts hydrogen atoms from the allylic carbon of the polymer chain. The site of a polymer chain that loses a hydrogen atom becomes a free radical. The two free radicals combine to form a crosslink. In addition, the primary free radical may also attack a double carbon–carbon bond on the polymer chain and initiate polymerization between adjacent double bonds on different chains, thus generating a small but densely crosslinked polymer cluster.[25] For simplification of the analyses in this study, we assume that all the crosslinks are uniformly distributed through the network and each DP molecule forms about 10 crosslinks on average.[26] Let C be the ratio of the number of DP molecules over the number of chains, so that each chain has about $N_c = 10C$ crosslinks. We have prepared a sample with the weight ratio of DP over the polymer being $r = 0.05$ PHR $= 5 \times 10^{-4}$. The molecular weight of DP is $M_{DP} = 270$ g mol^{-1}. For a kneaded sample, the molecular weight of the polybutadiene chains is assumed to be the same as that obtained, $M_w \sim 602\,000$ g mol^{-1}. Consequently, the number ratio of DP molecules over polymer chains is $C = rM_w/M_{DP} = 1.1$, and each polymer chain in the kneaded sample has about $N_c = 11$ crosslinks on average.

Rheology tests

We use a rheometer (DHR-3, TA Instruments) to test as-received, kneaded, and roll-milled polybutadiene, as well as their solutions. To characterize the dynamic viscoelasticity of polybutadienes, the polybutadienes are annealed for 12 hours at 65 °C and then cut into disks with a thickness of 0.6 mm and a diameter of 20 mm. A stainless steel parallel geometry with a diameter of 20 mm is used. The samples are compressed to a thickness of 500 μm and held for 30 min at 90 °C. A frequency sweep from 600 to 0.01 rad s^{-1} with a linear deformation strain of 1% at 25 °C is performed. To characterize the rheological behaviors of polybutadiene solutions, the polybutadienes are dissolved in phenyloctane to prepare 5% of the solutions. A cone plate geometry with a cone angle of 2°, a truncation gap of 59 μm, and a diameter of 60 mm is used. A flow sweep with a shear strain from 10^{-4} to 5×10^3 s^{-1} at 25 °C is performed to measure the steady state viscosity of polybutadiene solutions.

Tensile test

The stress–stretch curve, strength, loading–unloading curve, hysteresis, and residual stretch are measured by the uniaxial tensile test. Dogbone-shaped samples are made with dimensions of 20.0 × 4.0 × 0.6 (length × width × thickness, mm) in the gauge section. The real extension of the sample is recorded using a camera. The stress–stretch curve is measured to the fracture of the sample and the maximum stress is recorded as the strength. The loading–unloading curve is measured with a maximum stretch of three. We define hysteresis by the area between the loading and unloading curves divided by the area under the loading curve and residual stretch by the stretch when the stress vanishes during unloading.

Pure shear test

The stiffness, toughness, and fatigue threshold are measured by the pure shear test. The sample dimensions in the pure shear test are 63.5 × 1.0 × 0.6 (length × height × thickness, mm). Glass slides are used as the gripper and the sample is adhered to the glass slides using Krazy glue. The stiffness was calculated to be 0.75 of the initial slope of the stress–stretch curve. While measuring the toughness, an unnotched sample is stretched to obtain the strain energy density as a function of stretch, and a notched sample is stretched to fracture to obtain the critical stretch. The toughness was calculated as the product of the strain energy density at the critical stretch and the height of the undeformed sample. For the fatigue test, the strain energy density is measured from the stress–stretch curve of an unnotched sample after 2000 cycles of loading and unloading. For the fatigue fracture test, the crack growth is obtained by cyclic loading of a notched sample under a prescribed stretch. 50 000 cycles are performed for each test except when the crack driving force is too large or too small. The crack growth is observed under an optical microscope with a resolution of ~50 μm. The fatigue threshold is determined after 400 000 cycles of loading and unloading if we cannot detect any crack growth. Based on these conditions, the minimum crack growth that we can

detect is ~0.2 nm per cycle. All the mechanical tests are performed using a tensile tester (Instron 5966) and the fatigue fracture tests are performed using an in-house developed tester. The stretch rate is 0.1 s^{-1} for all the tests and the fatigue fracture test is performed at a stretch rate of 1 s^{-1} so the tests can be completed within a reasonable period.

Conflicts of interest

The authors declare no conflicts of interest.

Acknowledgements

This work was supported by the National Science Foundation under MRSEC (DMR-2011754) and by the Air Force Office of Scientific Research (FA9550-20-1-0397).

References

1 S. Kohjiya and Y. Ikeda, *Chemistry, manufacture and applications of natural rubber*, Woodhead Publishing, 2021.
2 A. J. Licup, S. Münster, A. Sharma, M. Sheinman, L. M. Jawerth, B. Fabry, D. A. Weitz and F. C. MacKintosh, *Proc. Natl. Acad. Sci. U. S. A.*, 2015, **112**, 9573–9578.
3 J. E. Mark, B. Erman and M. Roland, *The science and technology of rubber*, Academic press, 2013.
4 E. Warrick, O. Pierce, K. Polmanteer and J. Saam, *Rubber Chem. Technol.*, 1979, **52**, 437–525.
5 H. Fries and R. Pandit, *Rubber Chem. Technol.*, 1982, **55**, 309–327.
6 A. Ahagon, *Rubber Chem. Technol.*, 1996, **69**, 742–751.
7 A. K. Bhowmick, *Polym. Rev.*, 1988, **28**, 339–370.
8 G. Lake and P. Lindley, *J. Appl. Polym. Sci.*, 1965, **9**, 1233–1251.
9 P. Lindley, *Int. J. Fract.*, 1973, **9**, 449–462.
10 G. Lake and A. Thomas, *Proc. R. Soc. London, Ser. A*, 1967, **300**, 108–119.
11 J. Kim, G. Zhang, M. Shi and Z. Suo, *Science*, 2021, **374**, 212–216.
12 G. Nian, J. Kim, X. Bao and Z. Suo, *Adv. Mater.*, 2022, 2206577.
13 S. Hassan and J. Kim, *J. Mech. Phys. Solids*, 2022, **158**, 104675.
14 K. Kempfer, J. Devémy, A. Dequidt, M. Couty and P. Malfreyt, *Macromolecules*, 2019, **52**, 2736–2747.
15 S. A. Vanapalli, S. L. Ceccio and M. J. Solomon, *Proc. Natl. Acad. Sci. U. S. A.*, 2006, **103**, 16660–16665.
16 G. Kraus and K. Rollmann, *J. Appl. Polym. Sci.*, 1964, **8**, 2585–2604.
17 T. C. Ransom, D. Roy, J. E. Puskas, G. Kaszas and C. M. Roland, *Macromolecules*, 2019, **52**, 5177–5182.
18 Y. Takahashi, Y. Isono, I. Noda and M. Nagasawa, *Macromolecules*, 1985, **18**, 1002–1008.
19 Z. Wang, C. Xiang, X. Yao, P. Le Floch, J. Mendez and Z. Suo, *Proc. Natl. Acad. Sci. U. S. A.*, 2019, **116**, 5967–5972.
20 V. Tvergaard and J. W. Hutchinson, *J. Mech. Phys. Solids*, 1992, **40**, 1377–1397.
21 M. Tao, S. Lavoie, Z. Suo and M. K. Cameron, *Extreme Mech. Lett.*, 2023, 102024.
22 S. Wang, S. Panyukov, M. Rubinstein and S. L. Craig, *Macromolecules*, 2019, **52**, 2772–2777.
23 M. L. Méndez-Hernández, J. L. Rivera-Armenta, U. Páramo-García, S. Corona Galvan, R. García-Alamilla and B. A. Salazar-Cruz, *Int. J. Polym. Sci.*, 2016, **2016**, 7239540.
24 X. Liu, T. Zhou, Y. Liu, A. Zhang, C. Yuan and W. Zhang, *RSC Adv.*, 2015, **5**, 10231–10242.
25 L. González, A. Rodriguez, A. Del Campo and A. Marcos-Fernandez, *Polym. Int.*, 2004, **53**, 1426–1430.
26 L. D. Loan, *J. Appl. Polym. Sci.*, 1963, **7**, 2259–2268.